01 May 1992

The Interaction of System Structure, Index, and Numerical Stability in Classes of Differential/Algebraic Systems

Mariesa Crow

Missouri University of Science and Technology, crow@mst.edu

The Interaction of System Structure, Index, and Numerical Stability in Classes of Differential/Algebraic Systems

Mariesa L. Crow
Department of Electrical Engineering
University of Missouri-Rolla
Rolla, MO 65401

Abstract

Systems which are difficult to solve numerically have always been considered to be ill–conditioned and their analysis has been somewhat neglected. Recent advances in DAE theory have established that, although high–index DAE systems pose some interesting challenges, they are not the anathema they were once thought to be. This paper will present several examples of DAE systems which arise in power systems and nonlinear circuit analysis and will discuss both the analytical and numerical challenges these systems pose.

1 Introduction

A differential/algebraic system may be modeled

$$0 = \hat{F}(\dot{y}, y, t) \tag{1}$$

where $\frac{\partial \hat{F}}{\partial \dot{y}}$ is singular and $\frac{\partial \hat{F}}{\partial y}$ may or may not be singular. Systems of differential/algebraic equations (DAEs) of this type arise in connection with power systems, singular perturbation theory, control theory, circuit simulations, robot dynamics, and many other applications in the field of electrical engineering [1]. Only recently has concerted effort been put forth to find methods to numerically solve these systems [1]-[4]. Previously, systems of DAEs were frequently restated as ODEs, often with considerable difficulty or by destroying the structure of the problem (i.e., the resulting variables often no longer represent physical quantities, or the inherent sparsity of the system is destroyed) [2], but as DAE systems arise more and more frequently, it has become necessary to develop numerical methods for solving these systems distinct from the traditional methods for ODEs. If $\frac{\partial \hat{F}}{\partial \dot{y}}$ is invertible, this is a sufficient, but not necessary, condition for the system of (1) to be index one. If $\frac{\partial \hat{F}}{\partial \dot{y}}$ is non–invertible, the system is said to be of *higher* index [3]. Difficulties in using ODE methods for solving DAE systems occur when the systems have index greater than or equal to two.

Within the power system community this area was recently reaffirmed as an area of great interest. The application of limiters to mathematical models of physical devices may in some cases increase the index of the original system, which, in turn, may introduce numerical instabilities. When an independently varying state hits or exceeds a predefined limit, the system, in essence, loses at least one degree of freedom. This may manifest itself as an increase in the index of the system. Most current circuit simulators are not well equipped to handle such a change in system structure. The question of how to numerically simulate such a phenomena is still an open question. This paper will first discuss the change in the system index due to the inclusion of a parameter limiter, and will secondly discuss a numerical instability which may arise when systems of DAEs are simulated at points near dynamic bifurcation.

2 Limiters and System Index

The simulation of power systems usually involves numerically solving large stiff systems of differential/algebraic equations of the form:

$$\dot{x}(t) = F(x, y, \mu) \tag{2}$$
$$0 = G(x, y, \mu) \tag{3}$$

where x is the vector of states governing the dynamic behavior of the generator, y represents the vector of algebraic variables describing the behavior of the interconnecting network, and μ is a vector of time-varying inputs to the system. More specifically, consider the system shown in Figure 1 where the generating unit, modeled as a two axis model with an IEEE type I AVR/exciter is connected to an infinite bus, modeled as a constant voltage source. The dynamic model and network equations are given by [5]

$$\dot{\delta} = \omega - \omega_s \tag{4}$$
$$\dot{\omega} = \frac{w_s}{2H}\left(T_m - \left[E'_q - x'_d I_d\right] I_q - \left[E'_d + x'_q I_q\right] I_d - D(\omega - \omega_s)\right) \tag{5}$$
$$\dot{E}'_q = \frac{1}{T'_{d_0}}\left(-E'_q - \left(x_d - x'_d\right) I_d + E_{fd}\right) \tag{6}$$
$$\dot{E}'_d = \frac{1}{T'_{q_0}}\left(-E'_d + \left(x_q - x'_q\right) I_q\right) \tag{7}$$
$$\dot{E}_{fd} = \frac{1}{T_E}\left(-K_E E_{fd} + V_R\right) \tag{8}$$
$$\dot{R}_f = \frac{1}{T_F}\left(-R_f + \frac{K_F}{T_F} E_{fd}\right) \tag{9}$$
$$\dot{V}_R = \frac{1}{T_A}\left(-V_R + K_A R_f - \frac{K_A K_F}{T_F} E_{fd} + K_A\left(V_{ref} - V_t\right)\right) \tag{10}$$
$$0 = \left(R_s + R_e\right) I_d - \left(x_q + x_{ep}\right) I_q + V_s \sin\left(\delta - \theta_{vs}\right) \tag{11}$$
$$0 = \left(R_s + R_e\right) I_q + \left(x'_d + x_{ep}\right) I_d - E'_q + V_s \cos\left(\delta - \theta_{vs}\right) \tag{12}$$
$$0 = -V_d + R_e I_d - x_{ep} I_q + V_s \sin\left(\delta - \theta_{vs}\right) \tag{13}$$
$$0 = -V_q + R_e I_q - x_{ep} I_d + V_s \cos\left(\delta - \theta_{vs}\right) \tag{14}$$
$$0 = V_t - \sqrt{V_d^2 + V_q^2} \tag{15}$$

Several problems in engineering and physics result in systems which have an index greater than one. Under normal operating mode, power systems are generally considered to have an index of one. The system as described has an index of one: that is, $\frac{\partial G}{\partial y}$ (as described in (3) and as applied in (11) through (15)) is nonsingular. In some situations, however, the index of the system may be increased by the inclusion of a limiting constraint. The following example is one such situation.

In most applications V_{ref} (see (10)) is an input into the system, and the terminal voltage V_t is allowed to change dynamically. In some applications, however, it might be desired

0-7803-0593-0/92 $3.00 1992 IEEE

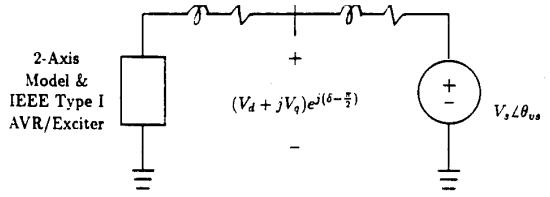

Figure 1: Simple Power System Model

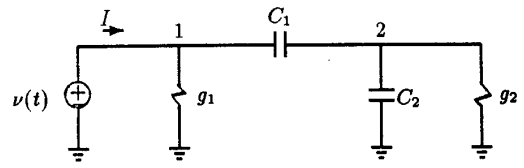

Figure 2: Index Two Floating Capacitor Circuit Example

to limit or constrain the terminal voltage to some constant value or trajectory by dynamically altering the reference voltage V_{ref}. To numerically determine the shape of this desired function, the additional constraint equation is added to the system and V_{ref} is allowed to change dynamically:

$$V_t = f(t) \quad (= 1.0\ pu \quad \text{for example}) \tag{16}$$

This altered system has an index of two. By constraining V_t, this disallows one "degree of freedom" in the differential or "state" variables, even though V_{ref} is now allowed to change. This subsequently would manifest itself by having only five differential states in the canonical system, whereas the system appears to have six differential states. Thus, in numerically solving this system with V_{ref} as a variable instead of V_t, the "static" portion of this system is now singular. This does not mean however, that the problem itself is ill-conditioned, only that care in the numerical solution process is necessary. In fact, this problem is numerically solvable if the following condition is satisfied

$$det \begin{bmatrix} I - \lambda \frac{\partial F}{\partial x} & -\lambda \frac{\partial F}{\partial y} \\ \frac{\partial G}{\partial x} & \frac{\partial G}{\partial y} \end{bmatrix} \neq 0 \text{ for some } \lambda \tag{17}$$

where λ is related to the integration stepsize h, at each stepsize h of interest. Thus, just because $\frac{\partial G}{\partial y}$ is not invertible, does not imply that the system is ill-conditioned, but may simply be of higher index. The numerical ramification of this analysis is that the set of differential and algebraic equations may no longer be solved separately in an iterative approach, but must be solved simultaneously, with caution applied to the selection of the integration stepsize.

A second example of the relationship between index and limiters is illustrated by the simple two-node example shown in Figure 2, which is made up of two capacitors, two resistors, and an independent voltage source. The DAE system which describes this system is:

$$\begin{bmatrix} C_1 & -C_1 & 0 \\ -C_1 & C_1 + C_2 & 0 \\ 0 & 0 & 0 \end{bmatrix} \begin{bmatrix} \dot{V}_1 \\ \dot{V}_2 \\ \dot{I} \end{bmatrix} = \begin{bmatrix} -g_1 & 0 & 1 \\ 0 & -g_2 & 0 \\ 1 & 0 & 0 \end{bmatrix} \begin{bmatrix} V_1 \\ V_2 \\ I \end{bmatrix} + \begin{bmatrix} 0 \\ 0 \\ -1 \end{bmatrix} \nu(t) \tag{18}$$

The algebraic equation

$$V_1 = \nu(t) \tag{19}$$

may be interpreted as a limiting constraint. Even though there appears to be a dynamic equation which describes the behavior of $\dot{V}_1$, V_1 is not an independent state - thus one degree of freedom is lost and this system has an index of two. Numerical problems may be encountered if the limiting constraint is placed dynamically, i.e., if a dynamic state hits a limit during the simulation process, and the integration procedure is not flexible enough to account for the change in index. An excellent discussion of the numerical solution of DAEs may be found in [1].

3 Numerical Instability

In the previous section, the interaction of system structure and index was discussed. In this discussion it was stressed that an increase in system index does not necessarily result in numerical instability if proper precautions are taken. In this section, a case of numerical instability due to a change in system structure will be presented.

For the purposes of this discussion, consider the two machine, three bus system shown in Figure 3. The dynamic equations for each machine in the system are as given for the one machine in (4)-(10), except that V_t is now replaced by V_i for $i = 1, 2$.

$$V_i \cos\theta_i + R_{s_i}\left(I_{d_i} \sin\delta_i + I_{q_i} \cos\delta_i\right) - x'_{d_i}\left(I_{q_i} \sin\delta_i - I_{d_i} \cos\delta_i\right) - \left[E'_{d_i} \sin\delta_i + \left(x'_{q_i} - x'_{d_i}\right) I_{q_i} \sin\delta_i + E'_{q_i} \cos\delta_i\right] = 0 \tag{20}$$

$$V_i \sin\theta_i + R_{s_i}\left(I_{q_i} \sin\delta_i - I_{d_i} \cos\delta_i\right) + x'_{d_i}\left(I_{d_i} \sin\delta_i + I_{q_i} \cos\delta_i\right) - \left[E'_{q_i} \sin\delta_i - \left(x'_{d_i} - x'_{q_i}\right) I_{q_i} \cos\delta_i - E'_{d_i} \cos\delta_i\right] = 0 \tag{21}$$

The algebraic constraints (11)-(15) are replaced by

$$V_i\left[I_{d_i} \sin(\delta_i - \theta_i) + I_{q_i} \cos(\delta_i - \theta_i)\right] - \sum_{k=1}^{3} V_i V_k \left(g_{ik} \cos\theta_{ik} + b_{ik} \sin\theta_{ik}\right) = 0 \tag{22}$$

$$V_i\left[I_{d_i} \cos(\delta_i - \theta_i) - I_{q_i} \sin(\delta_i - \theta_i)\right] - \sum_{k=1}^{3} V_i V_k \left(g_{ik} \sin\theta_{ik} + b_{ik} \cos\theta_{ik}\right) = 0 \tag{23}$$

for $i = 1, 2$. The network equations are given by

$$P_3 - \sum_{k=1}^{3} V_3 V_k \left(g_{3k} \cos\theta_{3k} + b_{3k} \sin\theta_{3k}\right) = 0 \tag{24}$$

$$Q_3 - \sum_{k=1}^{3} V_3 V_k \left(g_{3k} \sin\theta_{3k} + b_{3k} \cos\theta_{3k}\right) = 0 \tag{25}$$

The machine and excitation systems are modeled identically. The parameter data and steady state values for an initial loading of $P_3 = 2.5, Q_3 = 1.25$ are summarized in Tables 1 and 2 respectively.

For the case in question, the loading on the system is shown in Figure 4. The reactive loading is such that a constant power factor (i.e. P/Q = constant) is maintained. The system response to this change in loading was simulated using the trapezoidal method with a constant stepsize. The simulation results for a stepsize of $h = 0.005s$, $h = 0.015s$, and $h = 0.03s$ are shown above in Figures 5, 6, and 7, respectively. Note that Figures 5 and 7 are identical, whereas the results in Figure 6 depict a deviation from the normal course of simulation. Figure 6 is superimposed on a "correct" simulation using a stepsize of $h = 0.015s$ in Figure 8 (how this "correct" waveform was obtained will be discussed in length shortly). The region between

Table 1: Machine and excitation system data

parameter	value
H (sec)	10.0
D (pu)	1.00
x_d (pu)	0.90
x'_d (pu)	0.10
x_q (pu)	0.85
x'_q (pu)	0.10
T'_{d_0} (sec)	8.00
T'_{q_0} (sec)	0.25
K_A (pu)	25.0
T_A (sec)	0.20
K_E (pu)	1.00
T_E (pu)	0.35
K_F (pu)	0.05
T_F (pu)	0.35

Table 2: Initial operating states

variable	machine 1	machine 2
V (pu)	1.00	1.05
θ (rad)	0.00	-0.0183
δ (rad)	0.934	0.3280
ω (rad/sec)	377	377
E'_q (pu)	0.7108	1.1521
E'_d (pu)	0.7097	0.3144
E'_{fd} (pu)	1.6436	2.4676
V_R (pu)	1.6436	2.4676
R_F (pu)	0.2348	0.3525
V_{ref} (pu)	1.065	1.1487
T_M (pu)	1.500	1.000
P_{gen} (pu)	1.500	1.000
Q_{gen} (pu)	-0.0682	1.4746

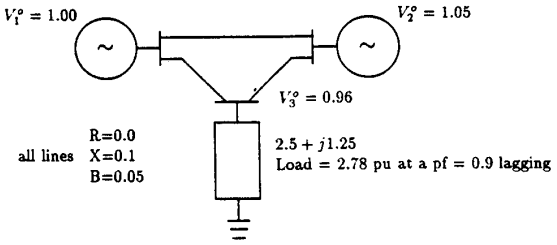

Figure 3: Example Test System

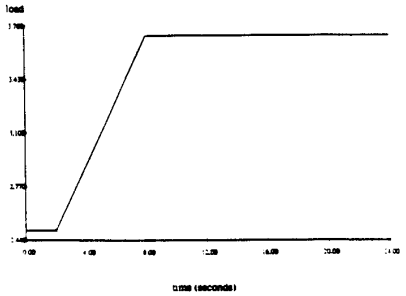

Figure 4: Loading at bus #3

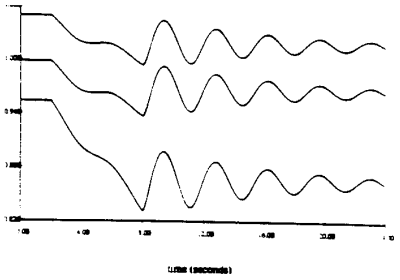

Figure 5: Simulation results for $h = 0.005s$

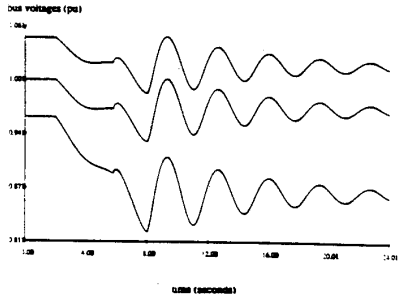

Figure 6: Simulation results for $h = 0.015s$

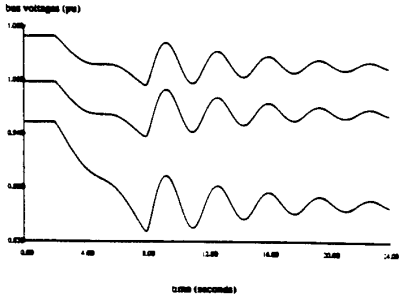

Figure 7: Simulation results for $h = 0.03s$

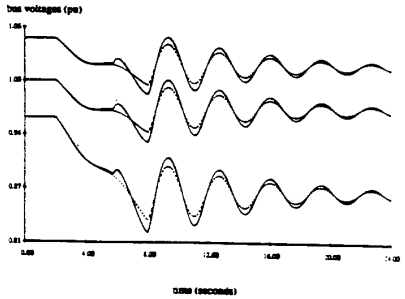

Figure 8: Superimposed simulation results for $h = 0.015s$

5.5 and 6.0 seconds is enlarged and shown in Figure 9. Note that before the deviation occurs, there is only a difference of 0.002 pu between the two waveforms (which is less that a quarter of a percent) In addition, note also that the two waveforms settle to the same steady-state value once the load obtains its final value.

It has been frequently documented that in steady state, there exist multiple equilibrium points for a particular loading value. In some instances, the steady state equilibrium exhibit both saddle node and Hopf bifurcations which give rise to small amplitude limit cycles [6]. It has also been documented that the equilibriums go through a period of instability as the load increases, but may settle to a stable equilibrium at a higher value of loading [7]. What appears to be occurring in the simulations

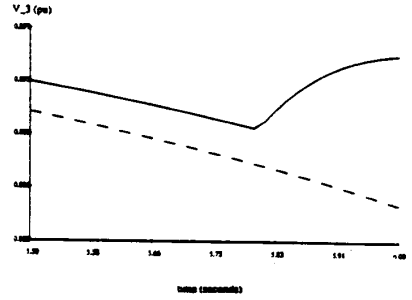

Figure 9: Enlargement of Figure 8

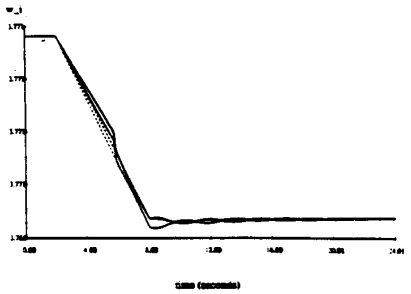

Figure 10: Superimposed angular frequencies

shown in Figures 6 and 8 is that two trajectories for the same loading reside very close in state space, and in the course of the numerical integration the solution waveform essentially jumps from one trajectory to another. They settle to the same steady state equilibrium, because for the final loading the multiple equilibria are sufficiently far apart that the trajectories are within the same region of attraction. This phenomenon is especially interesting if one is interested not only in the final resting point but in the *transition* from one loading to another. The simulation of Figure 6 would lead to erroneous conclusions concerning maximum voltage magnitude swings, etc.

One obvious question which has not yet been addressed is why this phenomenon appears only in the stepsize case $h = 0.015s$ and not in the other two (one smaller, one larger). This may be explained thusly: in the numerical solution of the discretized nonlinear equations, an iterative Newton-Raphson (NR) method is used. A convergence criteria of $\Delta x \leq \epsilon = 0.0025$ was used, where Δx is the update of all states, dynamic and static, in the system. For the stepsize $h = 0.005s$, the predictor step gave an initial guess sufficiently close to the correct solution such that, combined with the quadratic convergence properties of the NR method, one iteration-update was well within the cited criterion. For the stepsize $h = 0.03s$, the predictor guess was less accurate and thus, at least two iteration-updates were performed at each time step. Once again, the quadratic convergence properties of the NR method brought the mismatch well within the cited convergence criterion. The case of the stepsize $h = 0.015s$ falls into the "gray region" where, at each iteration-update, the error was on the order of ϵ - thus only one iteration-update at each time step was performed, allowing the solution to "drift" within an envelope of ± 0.0025 of the "true solution." When this envelope overlapped the envelope of the alternate solution, the jump occurred. There are several ways to protect one's simulation against this errant behavior. Firstly, one may select a smaller ϵ, forcing more iteration-updates per time step, or secondly, a more robust predictor method may be utilized. The first of these alternatives was employed to obtain the "correct" solution waveform depicted in Figure 8.

One final oddity of this phenomenon is that only the static states (bus voltages) deviate from the true solution waveform. The dynamic states actually jump back to the true waveform. Figure 10 illustrates the behavior of ω_i. This is not totally unexpected since the quadratic nature of equations (22)-(25) give rise to two voltage values for each dynamic state. At the particular instant in time when the deviation occurs, these voltage values are quite close.

4 Conclusions

This paper discussed two areas where the numerical stability of the simulation process is affected by the system behavior. In the first area, the inclusion of limiters was shown to increase the index of the system, but it was noted that although the Jacobian of the static portion of the DAE system becomes singular, this does not necessarily indicate numerical instabilities. It was shown that if the system is solvable there exists at least one stepsize h, such that the simultaneous Jacobian is invertible and thus no numerical instabilities exist.

In the second area, a stepsize dependent instability was analyzed. It was shown how the dynamic behavior of the system greatly affected this instability and a few suggestions to eliminate the instability were presented.

5 Acknowledgements

The author would like to thank E. Keith Stanek for several very valuable discussions. This work was supported under the National Science Foundation grant NSF-ECS-91-08914.

References

[1] K. E. Brenan, S. L. Campbell, L. R. Petzold, *Numerical Solution of Initial-Value Problems in Differential-Algebraic Equations*, Elsevier Science Publishing Co., Inc., New York, New York, 1989.

[2] B. J. Leimkuhler, *Approximation methods for the consistent initialization of differential-algebraic equations*, Report, no. UIUCDCS-R-88-1450, University of Illinois, Urbana, Illinois, August 1988.

[3] P. Lötstedt, L. Petzold, *Numerical solution of nonlinear differential equations with algebraic constraints I: Convergence results for backward differentiation formulas*, Mathematics of Computation, vol. 46, no. 174, pp. 491-516, April 1986.

[4] L. Petzold and P. Lötstedt, *Numerical solution of nonlinear differential equations with algebraic constraints II: Practical implications*, SIAM Journal of Scientific Statistical Computation, vol. 7, no. 3, pp. 720-733, July 1986.

[5] P. W. Sauer and M. A. Pai, *Modeling and Simulation of Multimachine Power System Dynamics*, Control and Dynamic Systems, edited by C. Leondes, vol. 43, pp. 1-59, 1991.

[6] E. H. Abed, et. al, *On Bifurcations in Power System Models and Voltage Collapse*, Proceedings of the 29th Conference on Decision and Control, Honolulu, Hawaii, December 1990, pp. 3014-3015.

[7] C. Rajagopalan, B. Lesieutre, P. W. Sauer, and M. A. Pai, *Dynamic Aspects of Voltages/Power Characteristics*, paper # 91 SM 419-2 PWRS, to appear in the IEEE Transactions on Power Systems.